Uranium 2010, Proceedings of the 3rd International Conference on Uranium, Saskatoon, Saskatchewan, Canada, August 2010, Vol. II, 177-187, Edited by E.K. Lam, J.W. Rowson, E. Özberk

THEORETICAL INVESTIGATION OF STRUCTURAL AND MECHANICAL PROPERTIES OF URANIUM OXIDES

B. Szpunar[1], J.A. Szpunar[2]

[1]*Department of Physics and Engineering Physics*
University of Saskatchewan
Saskatoon, Canada SK S7N 5A9

[2]*Department of Mechanical Engineering*
University of Saskatchewan
Saskatoon, Canada SK S7N 5A9

ABSTRACT

The changes of structural and mechanical properties of urania are investigated when it was oxidized to U_3O_8. The CASTEP *ab-initio* quantum mechanical program, employing density functional theory is used in this calculation. The total energy technique is implemented to investigate changes in the lattice constants. The *ab-initio* calculations predict a 36-38% increase in the volume per uranium atom when transforming from UO_2 to U_3O_8, which agrees very well with experimental data. The implication of this prediction on the linear expansion and fragmentation of fuel is discussed. The calculated elastic constants of urania are in good agreement with experiments. The predicted mechanical properties of UO_2 and U_3O_8 are compared.

INTRODUCTION

The following paper presents some preliminary research on the application of *ab-initio* calculations to assess changes in the properties of urania (UO_2) when it oxidises to U_3O_8. It is continuation of our first principles studies of nuclear fuels [1, 2]. The current study is of interest since the accidental ingress of coolant or air into the fuel-to-sheath gap may take place and cause a subsequent increase of the oxidation state of the fuel [3]. Deviations from stoichiometry can have a significant effect on several physical properties of UO_2 fuel [3] and they may play an important role in determining the thermal and mechanical behaviour of fuel following sheath failure. During the fuel oxidation process (especially in air), higher oxidation state oxides are formed with different lattice constants and structure. The crystal structure of these compounds is not easy to identify, and various models have been proposed by different groups [4]. The measurements for nonstoichiometric fuel are usually done at room temperature, and often rather complex structures are observed [5]. These structures and possible associated phase changes greatly affect the mechanical properties of the fuel, enhance or degrade the capacity of the fuel matrix to retain fission products and change fuel behaviour in the lattice [6, 7]. Knowledge of the lattice constants for higher oxidation state oxides of uranium is important in nuclear safety analysis since for example, the formation of U_3O_8 in a

defective element can cause cracks or even split the fuel sheath after disposal [8], because there is a net 38% volume increase when UO_2 is transformed into U_3O_8.

The current calculations are performed for temperatures of 0 K and idealized structures, where small unit cells are used. They are tractable by *ab-initio* methods, and the equilibrium structure is found by the total energy minimisation method. The CASTEP *ab initio* quantum mechanical program, employing density functional theory [9], is commonly used to study the structure of materials. The CASTEP code uses pseudopotentials, and it has been early demonstrated [10] that plane wave ultrasoft pseudopotentials predict structural properties of various compounds, containing lanthanides and actinides, in agreement with experiments. This high accuracy, first principle calculations do not require any experimental input other than the atomic number of mass of the constituent atoms and therefore have predictive capabilities.

It is of interest to study the effect oxidation and structure changes of uranium oxides on the elastic properties. Additionally according to Cottrell [11] the ratio of shear modulus (G) over bulk modulus (B) is related to the intrinsic brittleness of material. The atomistic theory interprets bulk modulus as the resistance (at small strains) to separation of the atoms while the shear modulus measures resistance to ductile sliding failure. Hence the criterion for intrinsic brittleness or ductility is measured by G/B ratio. According to Cottrell, for cubic metal and alloy crystals, the brittleness occurs when $G/B > 0.5$ and the ductility when $G/B < 0.4$ [11]. We will call such brittleness intrinsic because it does not take into account the presence of dislocations and various slip systems that are activated during deformation. The intrinsic brittleness will be calculated for stoichiometric urania (UO_2) and U_3O_8 compound.

ENERGIES, LATTICE CONSTANTS, CHARGES AND MAGNETIC PROPERTIES OF STOICHIOMETRIC URANIA AND U_3O_8

The structural optimization according to the Broyden–Fletcher–Goldfarb–Shanno (BFGS) (see e.g. [12]) of the total energy minimization is used. It can be determined, using iterative methods, when forces and stresses are minimized (almost vanish) within the total energy pseudopotentials method [9] and base on this the equilibrium lattice constants and the positions of atoms of stoichiometric urania are calculated (at 0 K). Our calculations for various uranium oxides were presented in Reference [1]. Here only UO_2 and U_3O_8 compounds are discussed. The implications of large volume expansion during oxidation to U_3O_8 are presented.

In Table 1 lattice constants for pure urania calculated using local exchange-correlation functional (LDA) [13] are compared with the results where the electronic exchange-correlation potential was approximated within the Generalized Gradient Approximation (GGA) framework [14, 15]. In contrast to the previous calculations [10, 2] where GGA was used with pseudopotentials developed for LDA, in this work PBE pseudopotentials developed for GGA [14, 15] are used. The lattice constant for stoichiometric urania shown in Table 1 calculated using GGA is larger (0.5472 nm) than calculated using LDA (0.5334 nm). The current calculations agree with the previously obtained values: 0.5458 nm [10], with the earlier version of the same software and 0.5446 nm [2]. The experimentally measured lattice constant of pure urania: 0.54582 nm [16], at 399 K temperature should be reduced by about 0.002 nm, to compensate for the thermal expansion, before they are compared with the value calculated at 0

K. The GGA [14, 15] calculations predict slightly larger lattice constant than the experiment, the value predicted by LDA [13] underestimate it.

The structure for U_3O_8, proposed by Loopstra [17] is shown in Figure 1. The CASTEP *ab initio* simulations predict that the $P\bar{6}2m$ structure proposed by Loopstra is stable. In Table 1, the results of spin polarized calculations are shown for this structure and for the stoichiometric urania. The magnetic moment of uranium atoms is about half (1.1 μ_B) of the value of the magnetic moment of uranium in UO_2. The calculated lattice constants (0.6864 nm (a), 0.4167 nm (c)) agree well with experimental measurements (0.6817 nm (a), 0.4145 nm (c)) and previously calculated values (0.6829 nm (a), 0.4145 nm (c)) [10]. Slightly larger lattice parameters, than calculated by us before (0.6827 nm (a) and 0.4152 nm (c) [1]), are presented here for GGA calculations (the PBE pseudopotentials were used). These values of the lattice constants lead to (Equation 1 gives relative change of volume υ) a 38% increase of the volume per uranium atom when UO_2 is transformed to U_3O_8.

$$\upsilon = \left(\sqrt{3}6^{-1} a^2_{U_3O_8} c\right) / \left(4^{-1} a^3_{UO_2}\right) \qquad (1)$$

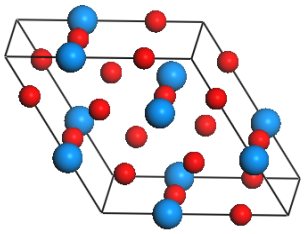

Figure 1 - Lattice structure of U_3O_8 (a), $P\bar{6}2m$ structure proposed by Loopstra [17]. Uranium and oxygen atoms are marked by spheres and larger radius spheres represent U atoms

This value is slightly larger than calculated before 36% [1], and estimated from Pickard et al. lattice constants ([10]: 37%).

In Table 1, the calculated charge transfer from uranium to the oxygen atoms is shown. The charge on oxygen atoms varies between –0.52 and –0.61 electrons, where lower charge transfer was observed for oxygen atoms in U_3O_8 ,where the unit cell volume is larger than in the stoichiometric urania. The calculated charge transfer on oxygen atoms is lower than the value of two electrons for a purely ionic compound, indicating that the uranium oxide bonding is partially covalent.

Table 1 - Lattice constants, spins, electronic charges on oxygen atoms and energies (per non-oxygen atom calculated using CASTEP [9]).

Compound	Structure	Energy per non-O atom [eV]	Magnetic state	Spin (U)	Spin (M)	Lattice constants [nm]	Charge (O) [electron]
UO_2	$Fm\bar{3}m$	-29.329	Paramagnetic	0		0.5361	-0.61
UO_2	$Fm\bar{3}m$	-30.709	Ferromagnetic	1.19		0.5472	-0.65
UO_2	$Fm\bar{3}m$	-30.709	Ferromagnetic (lda)	1.15		0.5334	-0.60
U_3O_8	$P\bar{6}2m$	-35.388	Ferromagnetic	0.55		0.6864 (a,b) 0.4167 ©	-0.58* -0.52# -0.57$

* - indicates the charge on oxygen atom in f position (0.748, 0, 0) (Figure 1)
# - indicates the charge on oxygen atom in q position (0.360, 0, 1/2) (Figure 1)
$ - indicates the charge on oxygen atom in c position (1/3, 2/3, 0) (Figure 1)

ELASTIC PROPERTIES

In this section details on elastic constants calculations are presented. The experimental values of elastic moduli pertain to a grain aggregate (where grains have randomly orientated crystallographic directions) rather than to single crystals. A completely random orientation of the grains was assumed in the computation. The formulas of Reuss [18] and Voigt [19] were employed in these computations, which provide least upper-bound and greatest lower-bound values for the aggregate. In particular, the approach by Voigt corresponds to averaging over the elastic constants (stiffness), where the following formulas for bulk modulus (B_V) and shear modulus (G_V) are obtained:

$$B_V = (A + 2B)/3, \qquad G_V = (A - B + 3C)/5 \tag{2}$$

where

$$\begin{aligned} 3A &= c_{11} + c_{22} + c_{33} \\ 3B &= c_{23} + c_{31} + c_{12} \\ 3C &= c_{44} + c_{55} + c_{66} \end{aligned} \tag{3}$$

and c_{ij} are elastic constants. The Reuss approach pertains to averaging over the elastic moduli (compliancies), where the formula for the bulk modulus (B_R) and shear modulus (G_R) is:

$$B_R = 1/(3a + 6b), \; G_R = 5/(4a - 4b + 3c) \tag{4}$$

in which:

$$\begin{aligned} 3a &= s_{11} + s_{22} + s_{33} \\ 3b &= s_{23} + s_{31} + s_{12} \\ 3c &= s_{44} + s_{55} + s_{66} \end{aligned} \quad (5)$$

Here s_{ij} are the elastic moduli (these are the elements of the inverse matrix of the elastic constants matrix with elements: c_{ij}). The final values of B and G (shown in Table 2) are calculated as an average of Voigt and Reuss (known as Hill approach):

$$B = (B_V + B_R)/2, \quad G = (G_V + G_R)/2 \quad (6)$$

Having calculated the bulk and shear modulus, the Young's modulus (Y) can be evaluated for an isotropic material or isotropic aggregate of grains having non-isotropic elastic properties as:

$$Y = 9BG/(3B + G) \quad (7)$$

Additionally Young modulus is calculated in [100] and [001] directions from the relation:

$$\begin{aligned} Y_{[100]} &= 1/s_{11} \\ Y_{[010]} &= 1/s_{22} \\ Y_{[001]} &= 1/s_{33} \end{aligned} \quad (8)$$

Elastic properties of UO_2, and U_3O_8

The elastic constants of UO_2 were previously calculated using CASTEP [10] and they are shown in Table 2 together with experimental data from the reference [20]. The results demonstrate that CASTEP *ab initio* calculations reproduce reliably elastic properties of UO_2. The results of calculations agree rather well with experimental data [20]. In the present work we repeated calculations of the elastic constants for urania using most recent version of CASTEP and the new calculations for U_3O_8 are also shown in Table 2.

The cutoff energy for elastic constants calculations for both oxides using CASTEP was 420 eV (with 14 extra bands) and the Monkhorst-Pack special wave-vectors [21] were used. The grid for UO_2 was the 8x8x8 and for U_3O_8 the 4x4x6 grid was used. Four (default) values of strain were applied: ± 0.3 %, ± 0.1%.

Table 2 – Comparison of the Elastic Properties of UO_2, and U_3O_8

Property (in GPa)	UO_2 Calculated using CASTEP [10]	UO_2 Calculated using CASTEP (LDA)	UO_2 Experimental [20]	U_3O_8 Calculated using CASTEP
B	170.1	229.1	208.9	164.1
G	70.3 (G_V)	104.9		56.9
G/B	0.41 (G_V/B_V)	0.46		0.35 (G_V/B_V = 0.45))
Y ($Y_{[100]}$, $Y_{[001]}$)	185.4 (Y_V)	273.0 (342.9)		151.8 (147.8, 503.5 [001])
c_{11}	318.2	411.9 (± 1.7)	389.3	263.8 (± 3.1)
c_{12}	96.0	137.7 (± 0.4)	118.7	174.8 (± 0.6)
c_{44}	43.1	87.6 (± 1.2)	59.7	26.7 (± 0.1)
c_{33}				506.3 (± 3.1)
c_{13}				25.0 (± 0.4)
n		0.2506		0.66([100], [010]), 0.06([001])

The notation in Table 2 is the same as in the previous table and n is Poisson ratio. Since in reference [10] only elastic constants are presented, the derived moduli G, Y and G/B are calculated using Voigt approach only. The intrinsic brittleness, calculated according to Cottrell's prescription (G/B) [11] is also shown. The Voigt ratios indicate that U_3O_8 is more brittle but opposite is true for Hill's ratio. Additionally U_3O_8 is not cubic and has very different structure than UO_2 therefore criterion for intrinsic brittleness may be different than that for stoichiometric urania. The large anisotropy (147.8 (in x, y directions), 503.5 (z direction)) was found for Young modulus, as shown in the last column of Table 2.

APPLICATION

The calculated volume expansion factor ($\upsilon = 1.36$) due to oxidation of UO_2 to U_3O_8 can be used for estimating the respective linear expansion factor. It is assumed, as observed experimentally [22], that U_3O_8 oxide formation starts at the fuel surface and progresses inwards (see Figure 2).

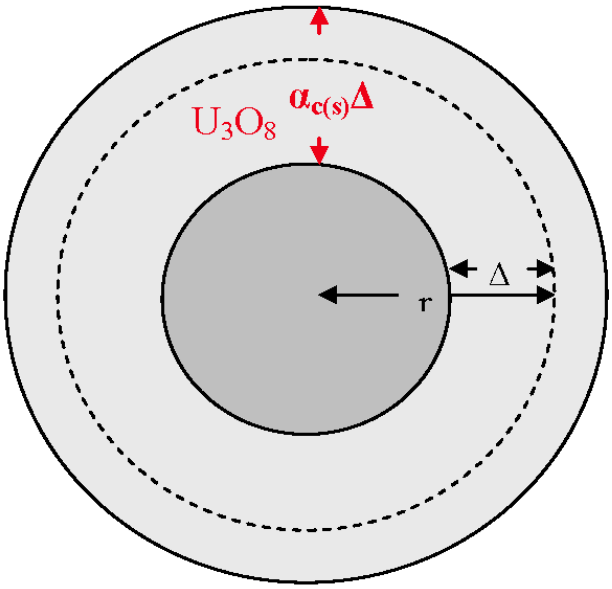

Figure 2 – Formation of U_3O_8 oxide on the UO_2 fuel surface is marked by light grey colour. The circle of radius r, of the initial unoxidised fuel sample, is shown by broken line and r indicates the initial radius of UO_2 core of cylinder, or sphere. Δ is equal to the thickness of UO_2 oxide that after oxidation to U_3O_8 oxide expands to $\alpha_{c(s)}\Delta$. $\alpha_{c(s)}$ indicates relative linear expansion for cylinder (c) or sphere (s), respectively .

We neglect in the present derivation thermal expansion and ignore the effect of possible cracks formation that often form at intermediate temperatures (900-1200ºC) [22]. At higher temperatures plastic deformation is observed, and at lower temperatures (500ºC) powderization occurs [22] during oxidation in air. Using simple geometrical considerations and assuming that volume expansion is uniform one can calculate the relative linear expansion factor of the urania that oxidised to U_3O_8 for a long cylindrical sample:

$$\alpha_c = \frac{\Delta - r + \sqrt{(r-\Delta)^2 + \Delta\upsilon(2r-\Delta)}}{\Delta} = \frac{\Delta/r - 1 + \sqrt{(1-\Delta/r)^2 + \Delta\upsilon(2-\Delta/r)}}{\Delta/r} \qquad (9)$$

with the following limits:

$\alpha_c = \upsilon$ for Δ = 0 (beginning of oxidation on the surface)

$\alpha_c = \sqrt{\upsilon}$ for Δ = r (whole sample oxidised to U_3O_8)

where r is the initial radius of UO_2 core of cylinder, Δ is equal to the depth of the original UO_2, oxide converted to U_3O_8 oxide, as shown in Figure 2.

Similarly for the spherical sample or the uniaxial cylinder one can get:

$$\alpha_s = \frac{\Delta - r + \sqrt[3]{(r-\Delta)^3 + \upsilon(r^3 - (r-\Delta)^3)}}{\Delta} = \frac{\Delta/r - 1 + \sqrt[3]{(1-\Delta/r)^3 + \upsilon(1-(1-\Delta/r)^3)}}{\Delta/r} \qquad (10)$$

with the following limits:

$\alpha_c = \upsilon$ for $\Delta = 0$ (beginning of oxidation on the surface)

$\alpha_c = \sqrt[3]{\upsilon}$ for $\Delta = r$ (whole sample oxidised to U_3O_8)

Infinite plane allows only for the expansion in the direction of oxide growth and therefore the linear expansion factor along this direction is equal to the volume expansion factor:

$$\alpha_p = \upsilon \tag{11}$$

The linear expansion factor for the same relative oxidation depth (Δ/r) is the same for fuels with different radii but the same shapes (cylindrical (Equation 9) or spherical (Equation10)). This is illustrated in Figure 3a. Knowing Young Modulus (Table 2) one can estimate the pressure on the walls of the tight container in which the immersed fuel oxidised to U_3O_8. The pressure is independent on the size of container but it varies with shape as it shown in Table 3.

Table 3 - Calculated stress in the tight container for urania oxidised to U_3O_8.

Young Modulus [GPa]	Stress [GPa] Sphere or equiaxial cylinder Strain: 0.10793	Stress [GPa] Long cylinder Strain: 0.16619	Stress [GPa] Plane Strain: 0.36
151.8 (random texture)	16.38	25.23	54.65
147.8 (x, y)	15.95	24.56	53.21
503.5 (z)	54.34	83.68	181.26

Many processes in fuel are controlled by the size of the surface area. In Figure 3a the relative changes in the length of fuel sample perpendicular to the surface area are shown as a function of the thickness of fuel sample that oxidized to U_3O_8. The linear expansion is the largest (Figure 3a) for samples with large (infinite) planar surfaces for which expansions takes place only in the direction of oxide growth. The measured experimental values (1.36 [8] and 1.32 [7]) for the highest expansion (υ) are comparable to the calculated here (1.38).

The predicted linear expansion for sphere is the same as for the equiaxial cylinder with the same radii (Equation 10). The cylindrical samples have height much higher than radius (Equation 9). The relative changes of the size of surface area are shown in Figure 3b.

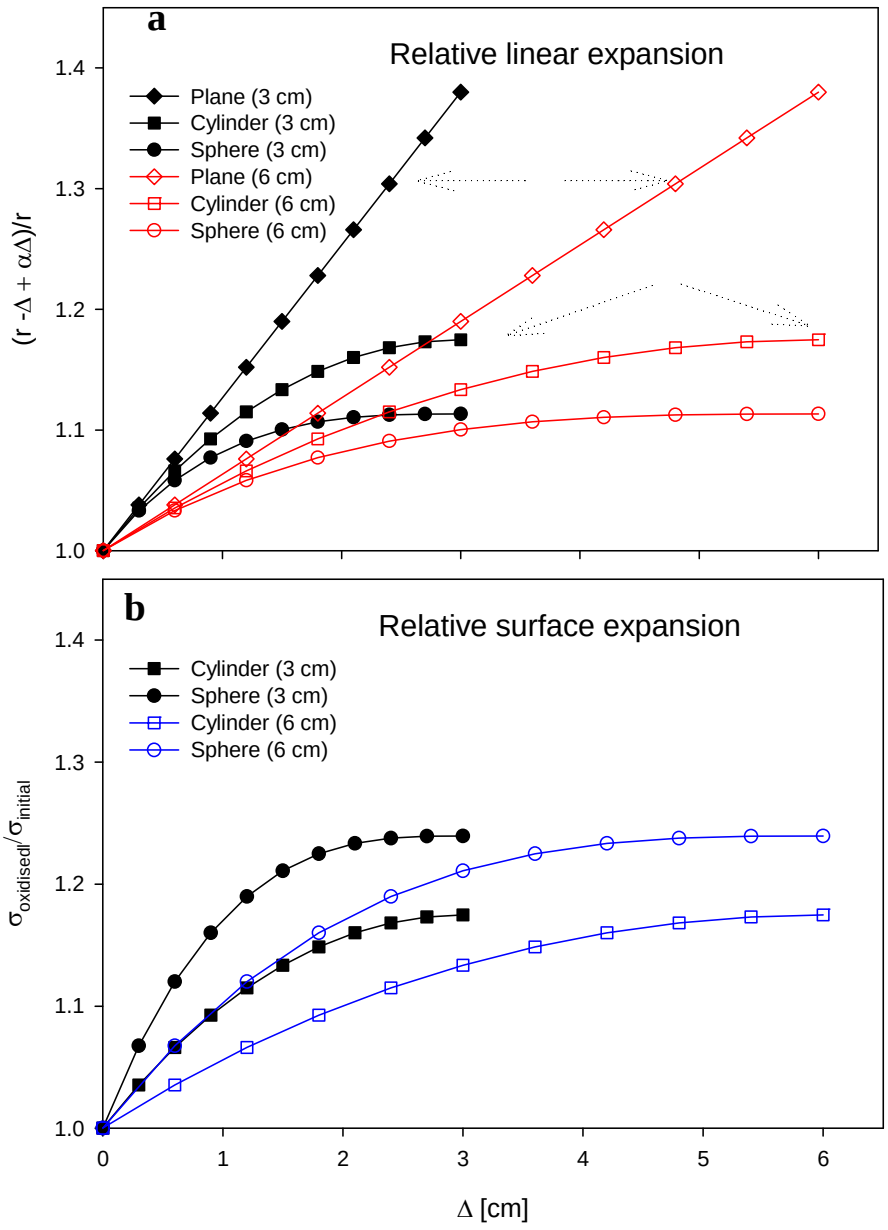

Figure 3 – (a) The relative changes in the length of the fuel, along the direction perpendicular to the surface of sample, as a function of the thickness of fuel sample that oxidized to U_3O_8. r is equal to the radius of the sphere or the cylinder while for plane it is equal to the initial thickness of the sample. The predicted linear expansion for sphere is the same as for the equiaxial cylinder with the same radii. The cylindrical samples have the height of cylinder much higher than the radius. (b) The relative changes of the size of surface area for the same samples as in (a). Surface area of infinite plane is not changed therefore relative surface expansion is equal to one and it is not plotted.

It may not have been realised before that the relative linear expansion, due to U_3O_8 oxide growth, is dependent on the shape of sample. Experimental measurements confirming these results would be useful. As shown in Figure 3b the calculated relative change of the surface area is the largest for the spherical sample and the area of large planar surfaces of the sample remains not changed (ratio equal to one).

At the intermediate temperatures (900-1200ºC) the large volume expansion of fuel may cause fragmentation. However the process is very complex and only idealised examples will be discussed here. Fragmentation causes significant increase of fuel surface area. Using geometrical evaluation it can be shown that the relative change in the total surface area ($\sigma_{fragmented}/\sigma_{initial}$) in the sample that breaks into n fragments with the same shape is:

$$\sigma_{fragmented}/\sigma_{initial} = n^{1/3} \qquad (12)$$

where $\sigma_{fragmented}$ is the total surface area of the fragmented sample and $\sigma_{initial}$ is the surface area of the sample before fragmentation occurs.

Even larger increase in the surface area would be observed if cylindrical sample breaks into cylindrical fragments that have all equal hight and the same basal plane as the original sample:

$$\sigma_{fragmented}/\sigma_{initial} = 1+(n-1)/(1+h/r) \qquad (13)$$

where r is the radius of the basal plane and h is the high of the sample before fragmentation. For equiaxial cylinder h = 2r and relative increase in the surface area is 1+(n-1)/3. For disks (h << r) the ratio is approximately equal to the number of fragments (n). In Figure 4 relative changes in surface area of the sample are shown for various number of fragments (calculated using Equations 12-13).

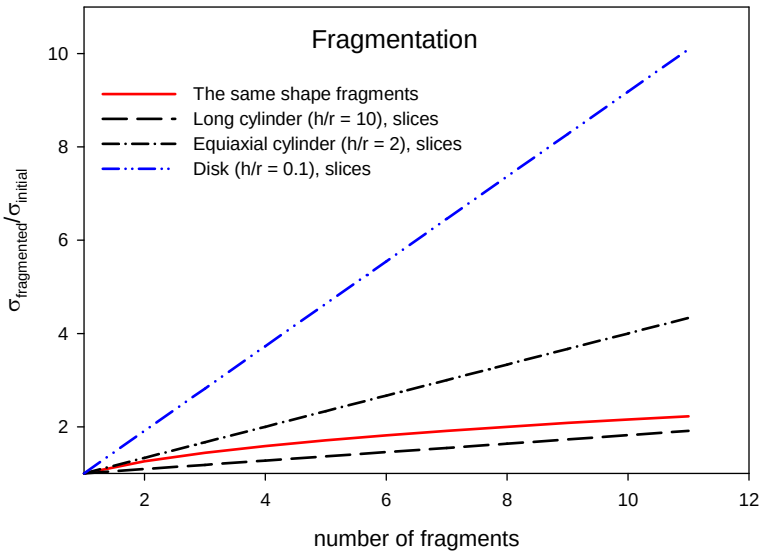

Figure 4 – Relative changes in the surface area of the sample as a function of the number of fragments (as indicated: solid line for Equation 12 and broken lines for Equation 13).

As it is illustrated in Figure 4 fragmentation may cause a significant increase in the surface area. The predicted increase is significantly higher than that shown in Figure 3b where the increase was related to the volume expansion.

CONCLUSION

Detailed calculations of the lattice structure and mechanical properties of UO_2 and U_3O_8 can complement experimental measurements, and they enhance understanding of the structural properties of fuel used in nuclear reactors. The *ab initio* calculations correctly predict a 36 % increase in the volume per uranium atom during transformation from UO_2 to U_3O_8. Also the magnetic and elastic properties of urania are well reproduced by simulations.

The linear expansion and the surface expansion caused by U_3O_8 oxide growth is calculated for various shapes of fuel. It may not have been realised before that the relative linear expansion, due to U_3O_8 oxide growth, is dependent on the shape of oxide sample. Experimental measurements confirming these results would be of interest.

The surface area increases during fragmentation of oxide and it is strongly dependent on the shape and the number of fragments; and it is much larger than the surface area increase due to volume expansion during oxidation.

The proposed calculation should be considered as an illustration of novel approach towards understanding of complex structural transformation and predicting changes of properties of nuclear materials. The methods that were applied, can be used for predicting structural transformation and properties of presently used nuclear materials and materials that are considered for applications in Generation IV nuclear reactors. We have developed comprehensive plan for future research on nuclear materials in different service environment. In addition to the presented here calculations for LDA and LDA + GGA approximations, the new functional (LDA +U), that improves calculations of band gaps and predictions of magnetic moments in strongly correlated systems, will be used in the future.

ACKNOWLEDGEMENT

This work was supported in part by a grant from the National Sciences and Engineering Research Council of Canada and by Atomic Energy of Canada Limited. The access to high performance supercomputers at McGill University is acknowledged.

REFERENCES

[1] B. Szpunar, J.A. Szpunar, "The Crystal Structure of pure and doped Urania", CNS 6th International Conference on Simulation Methods in Nuclear Engineering, Montreal, (2004 October 13-15), Conference Proceedings, (2004) 3C.

[2] B. Szpunar, J.A. Szpunar, "The Crystal structure and Elastic Properties of Pure and Dy Doped Urania", The 30th Annual Conference of the Canadian Nuclear Society, Calgary, Alberta, CANADA, May 31 - June 3 (2009), T3.

[3] B. Szpunar, B. J. Lewis, V. I. Arimescu, R. S. Dickson and L.W. Dickson., "Multi-component gas transport in the fuel-to-clad gap of candu fuel rods during severe accidents", J. Nucl. Mater., 294 (2001) 315-329.

[4] R.J. Ackermann, A.T. Chang and C.A. Sorrell, "Thermal Expansion and Phase Transformations of the U_3O_{8-x} Phase in Air", J. Inorg. Nucl. Chem., 39 (1977) 75-85.

[5] J.J. Katz, G.T. Seaborg and L.R. Morss (editors), "The Chemistry of the Actinide Elements", 2nd edition, Chapman and Hall, London, vol. 1 (1986) pages 256-267.

[6] J.C. Killeen and J.A. Turnbull, “An experimental and theoretical treatment of the release of ^{85}Kr from hyperstoichiometric uranium dioxide”, Proc. Workshop Chemical Reactivity of Oxide Fuel and Fission Product Release, Gloucestershire, England, eds. K.A. Simpson and P. Wood, Central Electricity Generating Board, April 7-9 (1987) 387-404.

[7] F.C. Iglesias, C.E.L. Hunt, F. Garisto and D.S. Cox, “Ruthenium release kinetics from uranium oxides”, Proc. International Center for Heat and Mass Transfer Conference on Fission Product Transport Processes in Reactor Accidents, Dubrovnik, Yugoslavia, May 22 – 26 (1989) 187-196.

[8] R.J. McEachern and P. Taylor, “A Review of the Oxidation of Uranium Dioxide at Temperatures Below 400°C “, J. Nucl. Mater., 254 (1998) 87-121.

[9] M.D. Segall, P.L.D. Lindan, M.J. Probert, C.J. Pickard, P.J. Hasnip, S.J. Clark and J.D. Payne, “First-Principles Simulation: Ideas, Illustrations and the CASTEP Code”, J. Phys. Cond. Matt., 14 (2002) 2717-2743.

[10] C.J. Pickard, B. Winkler, R.K. Chen, M.C. Payne, M.H. Lee, J.S. Lin, J.A. White, V. Milman and D. Vanderbilt, “Structural Properties of Lanthanide and Actinide Compounds within the Plane Wave Pseudopotential Approach”, Phys. Rev. Lett., 85 (2000) 5122-5125.

[11] D.G. Pettifor and A.H. Cottrell (editors), “Electron Theory in Alloy Design”, (see p.284), Ashgate Publishing, (1992) pp. 300.

[12] H. B. Schlegel, “Optimization of equilibrium geometries and transition structures” J. Comput. Chem., 1982, 3, 214-218 and references cited.

[13] D.M. Ceperley, B.J. Alder, B. J. "Ground State of the Electron Gas by a Stochastic Method", Phys. Rev. Lett., 45, (1980), 566-569.

[14] P. Perdew, Y. Wang, “Accurate and Simple Analytic Representation of the Electron-Gas Correlation Energy”, Phys. Rev. B45 (1992) 13244-13249.

[15] J.P. Perdew, K. Burke, M. Ernzerhof, M., "Generalized Gradient Approximation Made Simple", Phys. Rev. Lett., 77, (1996), 3865-3868.

[16] R.W.G . Wyckoff, Crystal Structures, ed. John Wiley & Sons, Inc., New York, Second Edition, vol. 2, (1963) pp. 467.

[17] B.O. Loopstra, “The Phase Transition in U_3O_8 at 210°C”, J. Appl. Cryst., 3 (1970) 94-96.

[18] A. Reuss, “Berechnung der FlieBgrenze von Mischkristallen auf Grund der Plastizitatsbedingung fur Einkristalle”, Z. Angew. Math. Mech. 9 (1929) 49-58.

[19] W. Voigt, “Lehrbuch der Krystallphysik” (ed. B.G. Teubner, Leipzig) (1928), pp. 962.

[20] I.J. Fritz, J., “Elastic properties. of UO_2 at high pressure”, Appl. Phys. 47 (1976) 4353-4357.

[21] H.J. Monkhorst and J.D. Pack, “Special points for Brillouin-zone integration”, Phys. Rev. B13 (1976) 5188-5192.

[22] D.S. Cox, F.C. Iglesias, C.E.L. Hunt, N.A. Keller, R.D. Barrand, J.R. Mitchell and R.F. O’Connor, “Oxidation of UO2 in Air and Steam with Relevance to Fission Product Releases”, Proc. Symp. On Chemical Phenomena Associated with Radioactivity Releases During Severe Nuclear Plant Accidents, Anaheim, CA, NUREG/CP-0078, Sept. (1986) 2.